# Appendix D

## The parton model

### D.1 Elastic electron scattering from nucleons

In the 1950s, experiments on elastic scattering of electrons from nucleon targets at rest in the laboratory revealed the electric charge distribution in protons and neutrons, clearly establishing the size of the nucleons.

The differential cross-section for the elastic scattering of electrons at high energies from a Dirac particle of mass $M$ and charge $e$ may be calculated in QED. To leading order in the fine-structure constant $\alpha = e^2/4\pi$, and neglecting the electron's mass compared with its energy, the differential cross-section for scattering from an unpolarised Dirac particle, initially at rest in the laboratory frame, in which the scattered electron emerges at an angle $\theta$ with respect to its incident direction, is

$$\frac{\mathrm{d}\sigma}{\mathrm{d}\Omega} = \frac{\alpha^2}{4E^2 \sin^4(\theta/2)} \left(\frac{E'}{E}\right) \left[\cos^2(\theta/2) + \frac{Q^2}{2M^2} \sin^2(\theta/2)\right], \tag{D.1}$$

where

$(E, \mathbf{p}) =$ initial electron energy-momentum four-vector,
$(E', \mathbf{p}') =$ final electron energy-momentum four-vector,
$q^\mu = (E - E', \mathbf{p} - \mathbf{p}') =$ energy-momentum transfer,
$Q^2 = -q_\mu q^\mu = (\mathbf{p} - \mathbf{p}')^2 - (E - E')^2$.

(See, for example, Gross, 1993, p. 294.)

Note that $Q^2$ is Lorentz invariant. For elastic scattering at a given energy, the angle $\theta$ determines, through energy and momentum conservation, all other quantities in the expression. For example,

$$Q^2 = 4EE' \sin^2(\theta/2), \tag{D.2}$$

where the energy $E'$ is given by

$$M(E - E') - 2EE' \sin^2(\theta/2) = 0 \tag{D.3}$$

(Problem D.1).

Taking $M$ to be the proton mass, the formula (D.1) does not fit the experimental data and, indeed, since the proton has an anomalous magnetic moment $\approx 1.79(e\hbar/2M)$, we



https://doi.org/10.1017/9781009401685.029 Published online by Cambridge University Press

would not expect a fit. More generally, the elastic scattering from an unpolarised 'extended' proton is of the form

$$\frac{\mathrm{d}\sigma}{\mathrm{d}\Omega} = \frac{\alpha^2}{4E^2\sin^4(\theta/2)}\left(\frac{E'}{E}\right)\left[\left\{f_1^2(Q^2) + \frac{Q^2}{4M^2}f_2^2(Q^2)\right\}\cos^2(\theta/2) + \frac{Q^2}{2M^2}\{f_1(Q^2) + f_2(Q^2)\}^2\sin^2(\theta/2)\right]. \tag{D.4}$$

The form of this expression is essentially determined given the proton has spin 1/2 and no electric dipole moment. $f_1(Q^2)$ is called the Dirac form factor of the proton, and $f_2(Q^2)$ is the form factor associated with the anomalous magnetic moment. At $Q = 0$, $f_1(0) = 1$ and $f_2(0) \approx 1.79$ (corresponding to the anomalous moment). The electric and magnetic form factors

$$G_E(Q^2) = f_1(Q^2) - \frac{Q^2}{4M^2}f_2(Q^2), \tag{D.5}$$

$$G_M(Q^2) = f_1(Q^2) + f_2(Q^2), \tag{D.6}$$

can be interpreted in the non-relativistic limit as Fourier transforms of the electric charge and magnetic moment distributions in the proton (Problem D.2). It is from their experimental determination that the size of the proton is inferred. Both $f_1(Q^2)$ and $f_2(Q^2)$ fall off rapidly as $Q^2$ increases (Fig. D.1). Similar form factors can be defined, and determined experimentally, for the neutron (using scattering data from deuterium targets). The analysis is consistent with the quark model. Since the electric charge is carried by the quarks, the charge and magnetic moment distribution should trace the distributions of quark charge and quark magnetic moment.

## D.2 Inelastic electron scattering from nucleons: the parton model

The early elastic scattering experiments were performed at electron energies $\leq 500\,\mathrm{MeV}$. Scattering at higher energies has thrown more light on the behaviour of quarks in nucleons, and revealed properties that will continue to be crucial for pursuing particle physics at the even higher energies of the future. Except where $Q^2$ is small, inelastic scattering, which involves hadron production, becomes the dominant mode at higher energies. In the case of inelastic scattering, $\theta$ and $E'$ are independent variables. In general, there are many other independent variables that describe the final hadronic system, but the very important differential cross-section $\mathrm{d}^2\sigma/\mathrm{d}E'\mathrm{d}\Omega$, called the *inclusive cross-section*, includes all the possible final hadronic states.

At the electron–proton collider HERA at Hamburg a beam of 30 GeV electrons meets a beam of 820 GeV protons head on. Many features of the ensuing electron–proton collisions are described by the *parton model.* which was introduced by Feynman in 1969.

In the parton model each proton in the beam is regarded as a system of sub-particles, called *partons.* These are quarks, antiquarks and gluons. Quarks and antiquarks are the partons that carry electric charge. The proton's energy and momentum $P^\mu$ is envisaged as being distributed over the different parton types $i$ with certain probability distributions. The mean number of partons of type $i$ in the proton carrying energy and momentum in the range $xP^\mu$, $(x + \mathrm{d}x)P^\mu$, $0 < x < 1$, is written $p_i(x)\mathrm{d}x$. Here the label $i$ covers all types of quarks, antiquarks and gluons (u, $\bar{\mathrm{u}}$, d, $\bar{\mathrm{d}}$, s, $\bar{\mathrm{s}}$, etc.). Scaling both energy and momentum by the same factor ensures that all the partons have the velocity of the proton. Any transverse momentum a parton may have is neglected. Thus, in the model, each proton in the HERA beam is regarded as a sub-beam of partons. The consequences of the model for

https://doi.org/10.1017/9781009401685.029 Published online by Cambridge University Press

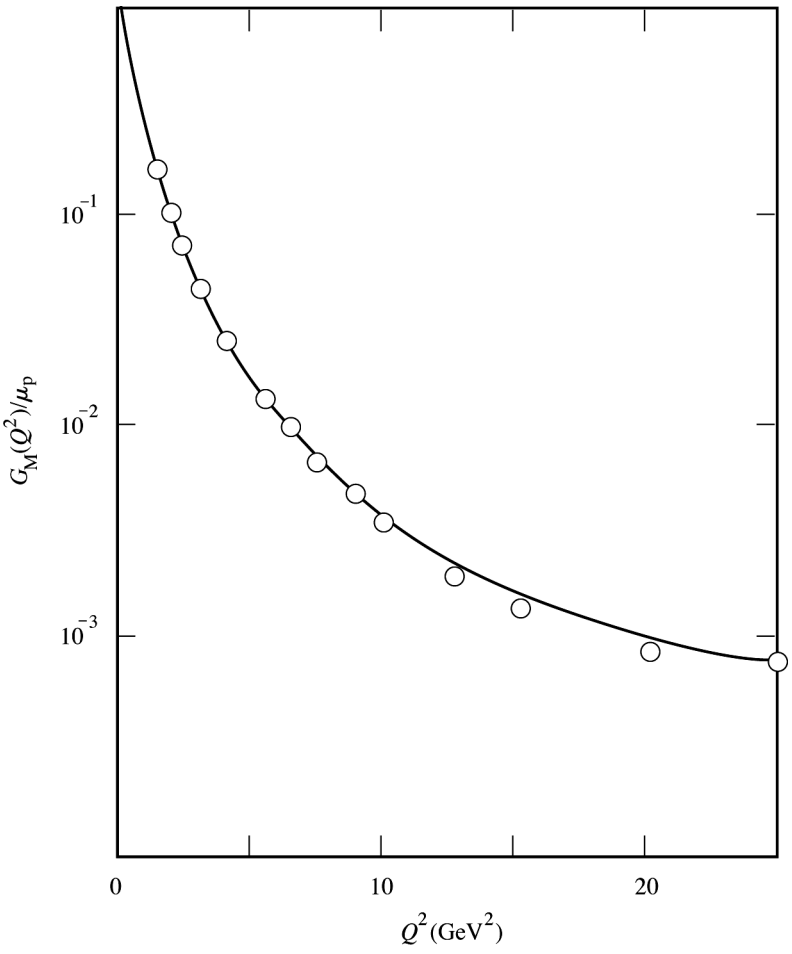


Figure D.1 This figure shows the measured magnetic dipole form factor of the proton. The data are quite well represented by the simple expression

$$G_{\mathrm{M}}(Q^2) = \mu_p \left[\frac{1}{1 + Q^2/\beta^2}\right]^2$$

with $\mu_p = 2.79$, $\beta = 0.84\,\mathrm{GeV}$. This curve is shown.

For $Q^2 < 3\,\mathrm{GeV}^2$, $G_{\mathrm{E}} = (Q^2)G_{\mathrm{M}}(Q^2)/\mu_P$ but for $Q^2 > 5\,\mathrm{GeV}^2$ only $G_{\mathrm{M}}(Q^2)$ can be measured with accuracy (see Coward *et al.*, 1968).

the inclusive cross-section can be most easily demonstrated in the rest frame of the proton. In this frame, a parton with energy–momentum fraction $x$ will behave like a particle of mass $xM$ at rest. For $Q^2 < M_{\mathrm{w}}^2$ the dominant scattering will be electromagnetic scattering from the charged partons: the spin $1/2$ quarks and antiquarks. For the elastic scattering from a parton of type $i$ with effective mass $xM$ we have

$$\frac{\mathrm{d}^2\sigma^i}{\mathrm{d}E'\mathrm{d}\Omega} = \frac{(xM)E}{E'}\delta\{(E' - E)(xM) + 2EE'\sin^2(\theta/2)\}\left(\frac{\mathrm{d}\sigma^i}{\mathrm{d}\Omega}\right)_{\mathrm{elastic}}, \tag{D.7}$$

https://doi.org/10.1017/9781009401685.029 Published online by Cambridge University Press

where $(\mathrm{d}\sigma^i/\mathrm{d}\Omega)_{\text{elastic}}$ is of the form given by (D.4), but with $M$ replaced by $(xM)$, and $\alpha^2$ by $q_i^2\alpha^2$ where $q_i^2 = (1/3)^2$ or $(2/3)^2$ depending on the type of parton. On integrating over $E'$, the $\delta$-function in (D.7) picks out the energy for elastic scattering through an angle $\theta$, as required by the condition (D.3) with $(xM)$ in place of $M$.
(Note that $\delta(aE' - b) = (E'/b)\delta(E' - b/a), a > 0$)). If we define

$$\nu = E - E'$$

then

$$\frac{\mathrm{d}^2\sigma^i}{\mathrm{d}E'\,\mathrm{d}\Omega} = \frac{(xM)E}{E'}\delta\{(xM)\nu - Q^2/2\}\left(\frac{\mathrm{d}\sigma^i}{\mathrm{d}\Omega}\right)_{\text{elastic}}. \tag{D.8}$$

Averaging over a large number of collisions, and assuming that the partons scatter incoherently, the inclusive cross-section in the parton model is

$$\begin{aligned}\frac{\mathrm{d}^2\sigma}{\mathrm{d}E'\,\mathrm{d}\Omega} &= \int \frac{(xM)E}{E'}\delta\{(xM)\nu - Q^2/2\}\left(\sum_i p_i(x)\left(\frac{\mathrm{d}\sigma^i}{\mathrm{d}\Omega}\right)_{\text{elastic}}\right)\mathrm{d}x \\ &= \frac{x}{\nu}\frac{E}{E'}\sum_i p_i(x)\left(\frac{\mathrm{d}\sigma^i}{\mathrm{d}\Omega}\right)_{\text{elastic}},\end{aligned} \tag{D.9}$$

where

$$x = Q^2/2M\nu, \tag{D.10}$$

and the sum is over all types of charged partons. Finally, inserting explicitly the general elastic scattering formula (D.4)

$$\frac{\mathrm{d}^2\sigma}{\mathrm{d}E'\mathrm{d}\Omega} = \frac{\alpha^2}{2ME^2\sin^4(\theta/2)}\left[\frac{M}{2\nu}F_2(x, Q^2)\cos^2(\theta/2) + F_1(x, Q^2)\sin^2(\theta/2)\right] \tag{D.11}$$

where

$$F_2(x, Q^2) = x\sum_i p_i(x)q_i^2\left\{\left(f_1^i\right)^2 + \frac{\nu}{2Mx}\left(f_2^i\right)^2\right\}, \tag{D.12}$$

$$F_1(x, Q^2) = \frac{1}{2}\sum_i p_i(x)q_i^2\left\{\left(f_1^i\right) + \left(f_2^i\right)\right\}^2 \tag{D.13}$$

(using (D.10), $Q^2/4x^2M^2 = \nu/2Mx$).

In fact the form (D.11) for the inclusive cross-section, in terms of two structure functions $F_1(x, Q^2)$ and $F_2(x, Q^2)$, is quite general, and does not depend on the model we have introduced.

The wavelength $\hbar/Q$ is a measure of the scale on which the structure of the proton is explored in an electron scattering experiment. For low $Q$, such that $\hbar/Q$ is large compared with the size of the proton, we can anticipate that the electron is scattered coherently from the proton as a whole. It is at high $Q$ that the parton model becomes interesting. For $Q^2 >$ a few GeV$^2$, incoherent parton scattering seems to dominate, and the quarks and antiquarks in the proton apparently behave almost like free elementary particles: their anomalous moments can be neglected and we can set $f_2^i = 0$. Then from (D.12) and (D.13)

$$F_2(x, Q^2) = 2xF_1(x, Q^2). \tag{D.14}$$

This, the *Callen–Gross relation*, is well satisfied experimentally.

If the charged partons are structureless Dirac particles, $f_1^i = 1$ for all $Q^2$, so that

$$F_2(x, Q^2) = x\sum_i p_i(x)q_i^2 = F_2(x), \tag{D.15}$$

$$F_1(x, Q^2) = \frac{1}{2}\sum_i p_i(x)q_i^2 = F_1(x), \tag{D.16}$$

https://doi.org/10.1017/9781009401685.029 Published online by Cambridge University Press

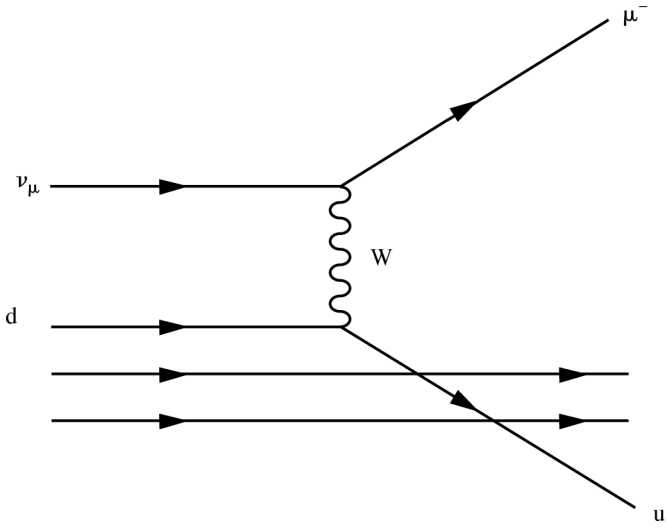


Figure D.2 An illustration of a muon neutrino converting to a muon on scattering from a d quark in a nuclean. The illustration indicates three 'valence quarks'. In fact there is additional scattering from quark–antiquark pairs that are generated by the gluon field.

and both $F_2$ and $F_1$ depend only on the dimensionless parameter $x = Q^2/2M\nu$. This is *Bjorken scaling*.

$F_2(x, Q^2)$ is illustrated in Fig. 17.3 over a wide range of values of $Q^2$ and $x$. It can be seen that the naïve parton model is not strictly correct, but that the $Q^2$ dependence is weak compared with that of the elastic form factor of the proton (Fig. D.1). It is usual to rewrite (D.12) as

$$F_2(x, Q^2) = x \sum_i p_i(x, Q^2) q_i^2, \tag{D.17}$$

associating the $Q^2$ dependence with the parton distribution itself rather than with the parton form factor. (See the discussion of the Altarelli–Parisi equations of QCD in Section 17.3.)

To determine the individual parton distributions $p_i(x, Q^2)$ introduced in equation (D.17) requires more information than is contained in the proton structure functions alone. The neutron has been investigated using deuteron targets, and, using the isospin symmetry between the neutron and proton (u $\leftrightarrow$ d, $\bar{\text{u}} \leftrightarrow \bar{\text{d}}$), the neutron data give further independent information. The weak interaction between quarks and leptons is described in Chapter 14. Neutrino and antineutrino inclusive cross-sections on proton and deuteron targets (Fig. D.2) give a further four independent relationships, so that, neglecting the contributions of heavier quarks, the individual u, d, s, $\bar{\text{u}}$, $\bar{\text{d}}$, $\bar{\text{s}}$ parton distributions can be estimated. In this approximation, (D.17) becomes

$$F_2(x) \approx \frac{4}{9}[xu(x) + x\bar{u}(x)] + \frac{1}{9}[xd(x) + x\bar{d}(x) + xs(x) + x\bar{s}(x)], \tag{D.18}$$

where $u(x) = p_{\text{u}}(x)$, etc.

https://doi.org/10.1017/9781009401685.029 Published online by Cambridge University Press

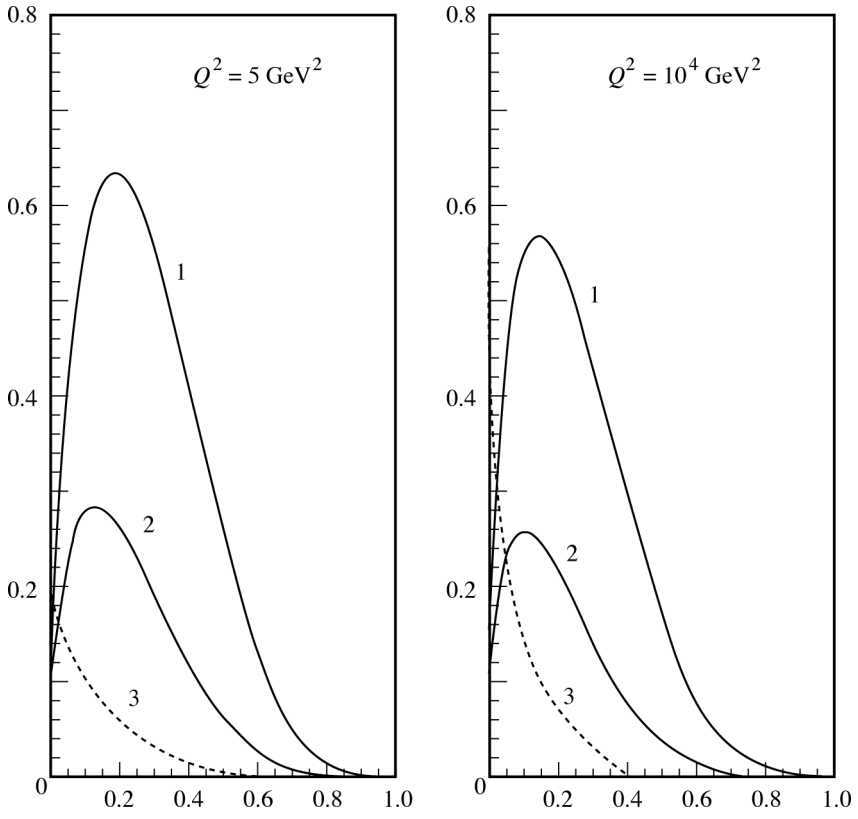


Figure D.3 Curve 1 is of $x(u(x) - \bar{u}(x))$ (see equation (D.18)). $u(x) - \bar{u}(x)$ is called the valence u quark distribution function. Curve 2 is $x(d(x) - \bar{d}(x))$, $(d(x) - \bar{d}(x))$, the valence d quark distribution function.

Curve 3 illustrates the sea quark distribution. Neglecting the generation of $c\bar{c}$, $b\bar{b}$ and $t\bar{t}$ pairs, curve 3 is of $x(\bar{u}(x) + \bar{d}(x) + \bar{s}(x))$.

Figure D.3 shows acceptable sets of parton distributions for the proton at $Q^2 = 5\ \text{GeV}^2$ and at $Q^2 = 10^4\ \text{GeV}^2$. With the present precision of the data these curves can be taken only as a fair indication of their forms. They have been constructed to satisfy the condition that the total parton charge is equal to $e$:

$$\sum_i \int_0^1 q_i\, p_i(x)\, \mathrm{d}x = 1,$$

but it is important to note that the charged partons carry only about one half of the total proton momentum:

$$\sum_i \int x p_i(x)\, \mathrm{d}x \approx 1/2.$$

The remainder is presumably carried by the electrically neutral gluons.

https://doi.org/10.1017/9781009401685.029 Published online by Cambridge University Press

### D.3 Hadronic states

The basic idea of the naïve parton model is that at high $Q^2$ an electron scatters from a free elementary quark or antiquark, and the scattering process is completed before the recoiling quark has time to interact with its environment of quarks, antiquarks and gluons. Thus in the calculation of the inclusive cross-section the final hadronic states do not appear.

In the model, at large $Q^2$ both the electron and the struck quark are deflected through large angles. Figure 1.10 shows an example of an event from the ZEUS detector at HERA. The transverse momentum of the scattered electron is balanced by a jet of hadrons that can be associated with the recoiling quark. Another jet, the 'proton remnant' jet is confined to small angles with respect to the proton beam. Events like these give further strong support to the parton model.

The 'deep inelastic' scattering data, when interpreted within the parton model, require the nucleon to have some $\bar{\mathrm{u}}$ and $\bar{\mathrm{d}}$ content, and also to contain $\mathrm{s}\bar{\mathrm{s}}$ quark-antiquark pairs (Fig. D.3). How is this to be reconciled with the simple quark model of nucleons at rest that we used in Chapter 1? A quark of the 'three quark' model of a nucleon, often called a *constituent quark*, is to be regarded as an elementary quark dressed with the strong interaction field, which will itself induce fluctuating quark–antiquark pairs. The quarks in the parton model are to be regarded as more like elementary quarks.

In quantum field theory, it is a non-trivial matter to make a Lorentz transformation on the internal wave function of a complex interacting system like a nucleon. The quark and gluon content of a proton are frame dependent. Because of time dilation, the time scale of the internal dynamics of the nucleon becomes long in a frame in which its momentum is large, and in this frame the parton distribution will be fixed over the time of interaction with an electron in a deep inelastic scattering experiment. The parton distributions in the model are taken to represent the distributions in this 'infinite momentum' frame.

### Problems

**D.1** Verify equations (D.2) and (D.3).

**D.2** In quantum mechanics, the differential cross-section for the elastic scattering of an electron with energy $E \gg m_\mathrm{e}$ from a fixed electrostatic potential $\phi(r)$ is given in Born approximation, and neglecting the effects of electron spin, by

$$\frac{\mathrm{d}\sigma}{\mathrm{d}\Omega} = \left(\frac{E}{2\pi}\right)^2 \left(e \int \phi(r)\, \mathrm{e}^{\mathbf{iq}\cdot\mathbf{r}} \mathrm{d}^3\mathbf{x}\right)^2,$$

where $\mathbf{q}$ is the difference between the initial and final wave vectors of the electron.

a. Show that $q = |\mathbf{q}| = 2E \sin(\theta/2)$, where $\theta$ is the scattering angle.

b. Poisson's equation relates the potential $\phi(r)$ to the charge density $\rho(r)$ by $\nabla^2\phi = -\rho$. Noting that $\nabla^2 \mathrm{e}^{\mathbf{iq}\cdot\mathbf{r}} = -q^2 \mathrm{e}^{\mathbf{iq}\cdot\mathbf{r}}$, and integrating by parts, show that

$$\frac{\mathrm{d}\sigma}{\mathrm{d}\Omega} = \left(\frac{E}{2\pi}\right)^2 \frac{1}{q^4} \left(e \int \rho(r)\, \mathrm{e}^{\mathbf{iq}\cdot\mathbf{r}} \mathrm{d}^3\mathbf{x}\right)^2.$$

Thus a measured cross-section can be used to infer the Fourier transform of the charge distribution, as this simple example illustrates.

D.3 Taking $Q^2$ and $\nu$ as independent variables instead of E′ and $\theta$, show that

$$\frac{\mathrm{d}^2\sigma}{\mathrm{d}E'\mathrm{d}\Omega} = \frac{1}{2\pi} \frac{\mathrm{d}^2\sigma}{\mathrm{d}E'\,\mathrm{d}(\cos\theta)} = \frac{EE'}{\pi} \frac{\mathrm{d}^2\sigma}{\mathrm{d}Q^2\mathrm{d}\nu}.$$

https://doi.org/10.1017/9781009401685.029 Published online by Cambridge University Press